Acta Cryst. (1996). D**52**, 115–123

Structure of a Complex Between Bulgecin, a Bacterial Metabolite, and Lysozyme from the Rainbow Trout

SOLVEIG KARLSEN AND EDWARD HOUGH*

Protein Crystallography Group, Institute of Mathematical and Physical Science, University of Tromsø, N-9037 Tromsø, Norway

(Received 20 March 1995; accepted 15 May 1995)

Abstract

Bulgecin, a sulfonated glycopeptide produced by *Pseudomonas acidophila* and *Pseudomonas mesoacidophila*, induces bulge formation and enhances lysis of bacterial cell walls when used in combination with β-lactam antibiotics. The compound does not itself exhibit any antibacterial activity, but has been shown to inhibit a soluble lytic transglycosylase (SLT70) from *Escherichia coli* which has a lysozyme-like domain. Recently, the crystal structure of an SLT–bulgecin complex has been determined to 3.5 Å resolution. We report here the crystal structure of a complex between lysozyme from the rainbow trout (RBTL) and bulgecin A at 2.0 Å resolution. As for the SLT–bulgecin complex, bulgecin is bound with the glycosaminyl moiety in subsite *C* and the proline residue in site *D* of the active-site cleft of RBTL, where it makes hydrogen-bonding interactions with the catalytic residues. The taurine moiety is bound to the left side of subsites *E* and *F* in the lower part of the active-site cleft. From the observed position of the bulgecin molecule, it seems reasonable that it is an inhibitor of rainbow trout lysozyme. The lysozymes may, in general, be a target for the design of a novel type of antibiotics distinct from the β-lactams which are insensitive to the muramidases.

1. Introduction

Bulgecins are sulfonated glycopeptides which, in cooperation with β-lactams, induce bulge formation and cell lysis in bacteria by enhancing the lytic activity of these antibiotics (Imada, Kintaka, Nakao & Shinagawa, 1982). Three classes of bulgecin have been isolated from cultures of *Pseudomonas acidophila* and *Pseudomonas mesoacidophila* and chemically characterized (Shinagawa, Maki, Kintaka, Imada & Asai, 1985). The structures of bulgecin A, B, and C are shown in Fig. 1 where they are numbered 1, 2, and 3, respectively. Bulgecin A, hereafter called bulgecin, is the main component. Each of the bulgecins consist of a sulfonated D-glucosamine unit linked to a proline ring (4-hydroxy-5-hydroxymethylproline) by a β-glycosidic linkage. Acid hydrolysis of bulgecin A and B yields taurine and β-alanine, respectively. The crystal structure of a desulfated derivative of bulgecin A has been determined (Shinagawa, Kasahara, Wada, Harada & Asai, 1984).

Murein (peptidoglycan), the biopolymer that envelops the whole bacterial cell as a single macromolecule, consists of glycan strands of variable length which are cross-linked by short peptide bridges to form a network-like structure (Rogers, Perkins & Ward, 1980). During bacterial growth and cell division, the cell wall polymer undergoes a balanced partial hydrolysis and resynthesis. For this purpose bacteria are equipped with a set of murein hydrolases, such as lysozymes and transglycosylases, and murein synthetases, such as the penicillin-binding proteins (PBP's) (Höltje & Schwarz, 1985). The latter are inhibited by penicillin and other β-lactam compounds. The lysozymes and transglycosylases are all muramidases, *i.e.* they selectively cleave the β-1,4-glycosidic bond between *N*-acetylmuramic acid (NAM) and *N*-acetylglucosamine (NAG) in the glycan strands. In addition, the transglycosylases perform an intramolecular muramyl transfer reaction to generate muropeptides with a 1,6-anhydromuramic acid (Höltje, Mirelman, Sharon & Schwarz, 1975).

Bulge formation in Gram-negative bacteria is believed to be a morphological change caused specifically by β-lactam antibiotics that interact with two penicillin-binding proteins (Spratt, 1975) which are responsible for peptide crosslinks in the peptidoglycan polymer (Waxman & Strominger, 1983). Bulgecin shows no antibacterial activity itself, but exhibits strong synergism with β-lactam antibiotics such as cefmenoxime and mecillinam (Imada *et al.*, 1982). Bulges formed by bulgecin combined with cefmenoxime are different in

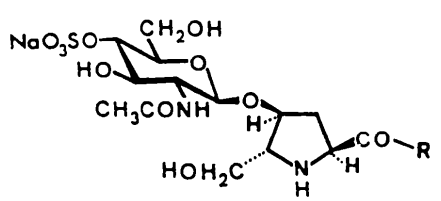

1 R = $NHCH_2CH_2SO_3H$
2 R = $NHCH_2CH_2CO_2H$
3 R = OH

Fig. 1. Structures of bulgecin A, B and C (numbered as 1, 2 and 3, respectively).

shape, size and rate of formation from those formed by mecillinam combined with cefmenoxime which implies that the bulge formation results from different mechanisms. Bulgecin appears, without affecting the PBP's, to lyse bacteria by damaging their cell surfaces after they already have been altered by β-lactam antibiotics (Nakao, Yukishige, Kondo & Imada, 1986).

Recently, the crystal structure of a soluble lytic transglycosylase (SLT70) from *E. coli* has been determined (Thunnissen *et al.*, 1994). This exomuramidase has a C-terminal domain with a lysozyme-like structure, although there is no significant sequence homology. The active-site cleft, which has been identified in this domain by analysis of a complex between SLT and bulgecin, contains similar features for substrate binding and cleavage as in lysozymes, although some striking differences are also observed (N. W. Isaacs, personal communication, 1994). The glycosaminyl moiety of bulgecin is bound to SLT in a site similar to subsite *C* in the active-site cleft of lysozymes. The proline moiety occupies a region analogous to subsite *D*. In an earlier study (Templin, Edwards & Höltje, 1992), SLT seemed to be inhibited by bulgecin.

From the X-ray analysis of the complex between SLT and bulgecin, it seemed likely that the bulgecin molecule should also bind to the active-site cleft of lysozyme. We have prepared crystals of a complex between lysozyme from the rainbow trout (*Oncorhyncus mykiss*) (RBTL) and bulgecin and solved the structure. The amino-acid sequence of RBTL (Dautigny *et al.*, 1991) and the structure determined at 1.8 Å resolution (Karlsen *et al.*, 1995), showed that it belonged to the *c*-type class of lysozymes. Two forms of this lysozyme, designated I and II, were found in the rainbow trout kidney (Grinde, Jollés & Jollés, 1988). In this paper we present results of the binding of bulgecin in the active-site cleft of the rainbow trout lysozyme.

Fig. 2. Ribbon drawing (*MOLSCRIPT*, Kraulis, 1991) of RBTL with a bulgecin molecule in the active-site cleft. The α-helices (H1–H4) are orange–green and the β-strands (B1–B3) are blue. C, O, N and S atoms in bulgecin are shown in grey, red, blue and yellow, respectively.

2. Experimental

2.1. *Cocrystallization of RBTL with bulgecin*

The two forms of the rainbow trout lysozyme, designated I and II, were purified as previously described (Grinde *et al.*, 1988). The bulgecin compound was kindly provided by Takeda Chemical Industries Ltd, Japan. The crystals were grown by the hanging-drop technique using a mixture of lysozyme and bulgecin. Well defined crystals suitable for X-ray structure studies, appeared after one to two weeks. The crystallization conditions were the same as for the native enzyme (Karlsen *et al.*, 1995) and the concentration of the bulgecin compound was 10 mg ml^{-1}. The crystals of the complex had the same appearance and size (up to 0.8 mm) as the native crystals, but the largest were more irregular in shape.

2.2. *Data collection and processing*

Intensity data from one crystal of the complex between RBTL and bulgecin were measured on a FAST area detector system with Cu $K\alpha$ radiation at room temperature. During the data collection, the FR571 SERIES 5 rotating-anode generator was operating at 40 kV and 70 mA and the program *MADNES* (Pflugrath, 1989) was used. The data set was collected using two goniometer settings with a rotation of 65° in ω for each scan. Reflections were measured with a crystal-to-detector distance of 60 mm and with a width of 0.1° for each individual rotation image. Cell parameters for the RBTL–bulgecin complex, seen in Table 1, are isomorphous with those for the native lysozyme ($a = b = 76.68$ Å and $\gamma = 54.46°$) collected on an R-AXIS II system (Karlsen *et al.*, 1995).

Processing of the data from the RBTL–bulgecin complex was carried out with *MADNES*, and profile-fitting with the program *XDS* (Kabsch, 1988). Merging to a unique data set was carried out using programs from the *CCP*4 software package (Collaborative Computational Project, Number 4, 1994). A summary of results from the data collection and merging is given in Table 1. A total of 10 895 unique reflections were measured to 2.0 Å resolution, giving a completeness of 86.1% and an $R_{\rm merge}$ of 5.9%.

2.3. *Refinement*

In common with the previously solved structures of complexes between the rainbow trout lysozyme and chito-oligosaccharides, the structure of the RBTL–bulgecin complex was determined by difference Fourier methods using phases obtained from the refined structure of native enzyme to 1.8 Å resolution (Karlsen *et al.*, 1995).

Five cycles of restrained least-squares refinement using *PROLSQ* (Hendrickson, 1985) with standard geometric restraints were carried out after removal of all solvent molecules from the active-site region of the native lysozyme model. An initial difference Fourier

Table 1. *Summary of results and conditions for the data collection*

Space group	$P3_121$
Cell parameters (Å)	$a = b = 76.57$, $c = 54.40$
Resolution range (Å)	14.68–2.00
No. of unique reflections ($\|F\| > 3\sigma_F$)	10895
Completeness (%)	86.1
R_{merge} (%)*	5.9

* $R_{merge} = \sum |I_i - \langle I \rangle| / \sum I_i$, where I_i is the intensity of an individual reflection and $\langle I \rangle$ is the mean intensity of that reflection.

map, $|F_{obs}(complex)| - |F_{calc}(native)|$, was calculated before a model of the bulgecin molecule was fitted into the electron density. The coordinates, obtained from the X-ray structure of a desulfated form of bulgecin A (Shinagawa *et al.*, 1984) and kindly provided by Takeda Industries Ltd, were used to generate initial coordinates for the inhibitor and in the restraints dictionary. The model was improved during the refinement by inspection and manual adjustment on an Evans & Sutherlands PS300 using the program *FRODO* (Jones, 1985). Omit maps were calculated for uncertain parts of the bulgecin molecule. After three rounds of successive positional and *B*-factor refinement and model building of the complex, the *R* factor had dropped to 16.3% for data from 8.0 to 2.0 Å resolution (see Table 2). During final refinement all atoms of the bound bulgecin molecule were refined with full occupancy. 110 water molecules were included in the final structure of the complex.

A summary of the final refinement statistics for both the native and the liganded structure of RBTL, is given in Table 2. The r.m.s. deviations from ideal values for the RBTL–bulgecin complex are 0.017 Å, 0.049° and 0.081 Å for bond lengths, angles and planar 1–4 distances, respectively. These values are smaller for the native structure, but the r.m.s. deviation of planar groups is 0.013 Å for both the liganded and the unliganded structure. High r.m.s. deviations for the planar 1–4 distances are also found for the complexes between RBTL and the chito-oligosaccharides (Karlsen & Hough, 1995).

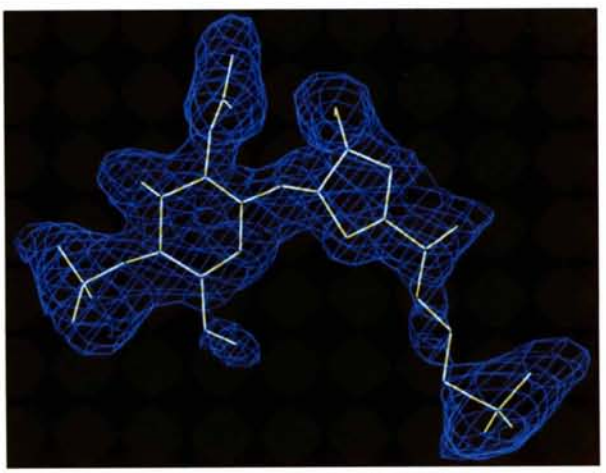

Fig. 3. Observed electron density ($|F_o| - |F_c|$ omit map), contoured at 0.12 e Å^{-3} for bulgecin bound in the active-site cleft of RBTL. Bulgecin was omitted from the coordinate file.

Table 2. *Summary of final refinement statistics for the native and the liganded structure of RBTL*

	Native RBTL	RBTL/bulgecin	St. dev.
Resolution range (Å)	8.0–1.8	8.0–2.0	
R factor*	0.174	0.163	
No. of reflections ($\|F\| > 3\sigma_F$)	16080	10895	
No. of protein atoms	999	999	
No. of ligand atoms	—	35	
No. of solvent atoms	127	110	
Deviations from ideal values			σ
Bond distances (Å)	0.013	0.017	0.02
Angle distances (Å)	0.044	0.049	0.04
Planar 1–4 distances (Å)	0.047	0.081	0.05
Planar groups (Å)	0.013	0.013	0.02
Chiral centers (Å^3)	0.038	0.041	0.06

* *R* factor $= \sum ||F_{obs}| - |F_{calc}|| / \sum |F_{obs}|$.

The coordinates for the structure of the RBTL–bulgecin complex have been deposited with the Protein Data Bank, Brookhaven National Laboratory, USA.*

3. Results and discussion

3.1. *Quality of the refined structure of the complex*

A Ramachandran plot of the structure of RBTL with bound bulgecin generated by the program *PROCHECK* (Laskowski, MacArthur, Moss & Thornton, 1993), shows that 92.9% of the main-chain dihedral angles fall within the most energetically favoured areas, whereas the remainder are found in additionally allowed regions. These values are similar to the native structure (Karlsen *et al.*, 1995) and for three complexes between RBTL and $(NAG)_2$, $(NAG)_3$ and $(NAG)_4$ (Karlsen & Hough, 1995). As in native RBTL and all of these complexes, Ser36, Tyr38, Gln57, Tyr62, Arg68, Asn74, Cys115 and Asn117 are also found in additional allowed regions for the RBTL–bulgecin complex. All these residues lie in loop regions which probably have a great deal of conformational freedom.

A Luzzati plot (Luzzati, 1952) shows that the mean error in atomic position is about 0.20 Å, comparable to the positional errors determined for the previously solved complexes with RBTL (Karlsen & Hough, 1995).

* Atomic coordinates and structure factors have been deposited with the Protein Data Bank, Brookhaven National Laboratory (Reference: 1LMC). Free copies may be obtained through The Managing Editor, International Union of Crystallography, 5 Abbey Square, Chester CH1 2HU, England (Reference: SE0176).

3.2. *Interpretation of the electron-density maps*

As is the case for native and oligosaccharide complexes of RBTL, the most poorly defined residues in the present complex also involve lysine, arginine, glutamine and asparagine side chains which lie on the surface of the protein molecule. Weak electron density and high temperature factors indicate that the side chains of residues Arg61, Lys73, Gln118, Asp119 and Arg121 exhibit a great deal of flexibility. In the active-site cleft of the lysozyme, well defined electron density is found for all residues that interact with the bulgecin molecule.

A final difference $(2|F_o| - |F_c|)$ map based on the refined structure of RBTL and bulgecin, clearly shows well defined electron density for a bulgecin molecule bound to the active-site cleft of the lysozyme. Fig. 2 illustrates the rainbow trout lysozyme in a ribbon drawing with bulgecin buried in the enzyme cleft. Fig. 3 shows the observed electron density for the bound bulgecin molecule contoured at 0.12 e Å^{-3} (2σ level), and average temperature factors for different parts of the molecule are given in Table 3. The atomic numbering scheme for bulgecin A is given in Fig. 4.

The *N*-acetylglucosamine ring of the bulgecin molecule is bound in site *C* in the same way as previously seen in the complexes between RBTL and chitin oligosaccharides (Karlsen & Hough, 1995). The proline ring of the bulgecin compound is bound in site *D*, approximately where we found the NAG unit at the reducing end of $(NAG)_3$ and $(NAG)_4$ molecules in the active site of RBTL. The 'tail' of the bulgecin molecule, *R* in Fig. 1, is pointing toward subsites *E* and *F* interacting with the well conserved three-stranded β-sheet region of the enzyme (Jollés & Jollés, 1984).

As found for the previously solved complexes between RBTL and chitin oligosaccharides (Karlsen & Hough, 1995) the NAG ring of the bulgecin molecule is tightly bound to site *C*. The buried 2-acetamido group which is known to play an important role in substrate specificity (Imoto, Johnson, North, Phillips & Rupley, 1972), has the lowest mean *B* factor (23.8 Å^2)

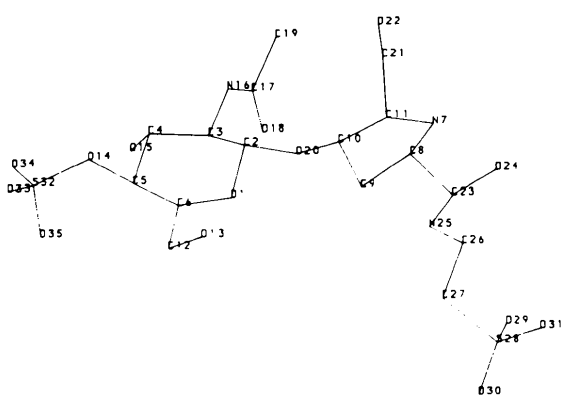

Fig. 4. Atomic numbering of the bulgecin molecule.

Table 3. *Average temperature factors for bulgecin bound to the active-site cleft to of RBTL*

Part of the bulgecin molecule	Average temperature factor (Å^2)
N-acetylglucosamine ring (O1, C2, C3, C4, C5, C6)	26.9
Proline ring (N7, C8, C9, C10, C11)	26.0
C3-acetamidoacetyl group (C17, O18, C19)	23.8
Hydroxymethyl group (C12, O13)	35.9
Hydroxymethyl group (C21, O22)	27.2
Sulfate group (S32, O33, O34, O35, O14)	31.8
Peptide group (C23, O24, N25, C26)	37.1
Sulfonyl group (S28, O29, O30, O31)	36.2
All atoms	30.3 +/− 5.3

for the whole molecule. The average temperature factors, however, for the ring atoms (19.0 Å^2) and 2-acetamido atoms (13.5 Å^2) of NAG ring *C* in the RBTL–$(NAG)_4$ complex are lower than in the bulgecin complex.

Poorly defined electron density and high average *B* factor (35.9 Å^2) are seen for the C6 hydroxymethyl group (C12, O13) of the NAG ring. This is exposed to solvent and is not hydrogen bonded to the protein. The observed electron density for the sulfate group (S32, O33, O34, O35, O14) on the C5 atom is diffuse and rather to be too 'flat' and 'elongated' to fit this group in a correct way.

Well defined electron density and a low average temperature factor (26.0 Å^2) for the atoms in the proline ring of bulgecin, shows that this also is highly ordered in the complex. The proline ring seems to be more strongly bound to the enzyme than the NAG ring in site *D* of the RBTL–$(NAG)_4$ complex which has a mean *B* factor of 34.3 Å^2 (Karlsen & Hough, 1995). One explanation for this can be that the proline residue carries a long taurine 'tail' which is hydrogen bonded to the protein, thus restraining the proline ring so that it is more strongly bound than NAG ring *D*. Another possibility is that the proline ring, which needs less space than the NAG unit, binds to this site with less strain. Well defined electron density and a low average temperature factor (27.2 Å^2) compared with the C6 hydroxymethyl group of the *C* NAG ring, is found for the C11 hydroxymethyl group of the proline ring. This is not unexpected since this group is involved in hydrogen-bonded interactions with the lysozyme.

Diffuse electron density and high *B* factors are seen for atoms C23, O24, N25, C26 and C27 which form of the long 'tail' of the bulgecin molecule. No density is present for the latter three atoms. More clearly defined electron density is, maybe due to hydrogen-bonded interactions, seen between the sulfonyl group at the end of the taurine moiety and the protein, but the temperature factors are higher than for the NAG and proline ring.

Table 4. *Geometry of the C–D glycosidic linkage*

Lysozyme	Sugar	φ ( )	ψ ( )
RBTL	$(NAG)_3$*	−121	−148
RBTL	$(NAG)_4$*	−113	−150
RBTL	bulgecin	−85	−114
HEWL	MGM†	−108	−110

* Values of φ and ψ are torsional angles about C(1)—O(4)′ [C(2)—O(22) for bulgecin] and O(4′)—C(4′) [O(20)—C(10) for bulgecin] defined by O(5)—C(1)—O(4′)—C(4′) and C(1)—O(4′)—C(4′)—C(5′) [O(1)—C(2)—O(20)—C(10) and C(2)—O(20)—C(10)—C(11) for bulgecin], respectively. † Values of the bound $(NAG)_3$ and $(NAG)_4$ in the active-site cleft of RBTL (Karlsen & Hough, 1995). ‡ Values of the bound NAM–NAG–NAM (MGM) in the active-site cleft of HEWL (Strynadka & James, 1991).

Table 5. *Endocyclic torsional angles of the NAG and proline ring in bulgecin*

Torsional angle	Unliganded bulgecin	Liganded bulgecin
C6—O1—C2—C3	−61	−56
O1—C2—C3—C4	54	63
C2—C3—C4—C5	−51	−50
C3—C4—C5—C6	51	30
C4—C5—C6—O1	−57	−23
C5—C6—O1—C2	64	37
N7—C8—C9—C10	−42	−41
C8—C9—C10—C11	44	46
C9—C10—C11—N7	−30	−32
C10—C11—N7—C8	3	4
C11—N7—C8—C9	24	25

Table 6. *Protein–ligand interactions in the complex of RBTL/bulgecin*

Bulgecin atom	Protein atom	Distance (Å)
N7	OD2 Asp52	2.88
O14	OW 241	3.27
O14	OW 150	3.07
O15	NE1 Trp63	2.87
N16	CO Ala107	3.17
O18	NH Asn59	2.83
O22	NH Val109	3.01
O22	OE2 Glu35	2.81
N25	OW 240	2.95
O30	OG1 Thr47	2.51
O30	NH Thr47	2.76
O31	ND2 Asn46	2.69
O33	OW 243	3.11
O34	OW 151	2.94

The 'tail' is, thus, the most flexible part of the bound bulgecin molecule.

3.3. *Geometry of bulgecin bound to RBTL*

The geometry of the β-glycosidic linkage between the NAG and the proline unit of bulgecin is detailed in Table 4. Values of the *C–D* bonding found in the complexes between RBTL and the tri- and tetra-oligomers of chitin (Karlsen & Hough, 1995) and the complex between hen egg-white lysozyme (HEWL) and NAM–NAG–NAM (MGM) (Strynadka & James, 1991), are included for comparison.

Crystal structure determinations of a number of oligosaccharides have shown that the glycosidic linkage, described by the torsional angles φ and ψ, varies from −71 to −96° in φ and −107 to −161° in ψ (Mo & Jensen, 1978; Jeffrey, 1990). Torsion angles for the bound bulgecin molecule are within these ranges, whereas the φ angles for the *C–D* linkage in the sugar complexes of RBTL and HEWL are outside the observed range for this parameter. Thus, the glycosidic linkage between the NAG and proline moieties in bulgecin exhibits less deviation from 'ideality' than the equivalent linkage in lysozyme–sugar complexes. One explanation for this may be that an unusual geometry of this glycosidic linkage is necessary for optimal adaptation of the sugar ring in subsite *D* in order to obtain the most effective hydrolysis of the substrate (Karlsen & Hough, 1995).

Table 5 lists the endocyclic torsion angles for the atoms associated with the NAG and proline ring in the liganded and unliganded structures of bulgecin. The pyranose ring of the enzyme-bound bulgecin molecule clearly deviates from the energetically favoured chair ($^4C_1$) conformation, but does not have a sofa conformation. The C3—C4—C5—C6, C4—C5—C6—O1 and C5—C6—O1—C2 dihedral angles are considerably smaller for this sugar ring than for the desulfated unbound structure of bulgecin and the NAG unit in site C in the complexes between the RBTL and the chito-oligosaccharides (Karlsen & Hough, 1995). The endocyclic torsional angles in the bound proline unit exhibit only small deviations from the equivalent angles in the unliganded ring. Comparison of the bond distances in the lysozyme-bound and free bulgecin molecule, shows that only minor changes have occurred upon binding to the active-site cleft.

Fig. 5, a superimposition of the structures of the free and the liganded form of bulgecin, indicates that the NAG and proline unit have moved relatively to each other with the largest conformational changes about the glycosidic linkage and not within the NAG and proline ring themselves. The taurine moieties of the bulgecin molecules are pointing in the same direction but with somewhat different conformations. The r.m.s. deviation between free and enzyme-bound bulgecin is 1.34 Å indicating that conformational differences clearly are imposed by interactions between the liganded molecule and the lysozyme.

3.4. *RBTL–bulgecin interactions*

Figs. 6(*a*) and 6(*b*) show hydrogen-bonding interactions between the rainbow trout lysozyme, bound water molecules and the bulgecin ligand in the active-site cleft. Protein–inhibitor interactions are detailed in Table 6. Bulgecin displaces eight ordered water molecules from the active-site cleft of native lysozyme.

It is not surprising that the NAG ring of bulgecin binds to subsite *C* since previously solved crystal structures of

complexes between various saccharides and lysozymes have shown this site to be most preferred binding site (Karlsen & Hough, 1995; Strynadka & James, 1991; Cheetham, Artymiuk & Phillips, 1992). Site *C*, which for steric reasons only can accommodate an NAG and not an NAM residue, seems to play a key role in the substrate recognition and cleavage specificity (in Imoto *et al.*, 1972).

The sulfonated *N*-acetylglucosamine ring in bulgecin forms three hydrogen bonds with the lysozyme molecule and three with bound water molecules. Two hydrogen-bonding interactions between the buried C3 acetamido group and RBTL are found between atoms N16 and O18 and the main-chain CO group of Ala107 and NH of Asn59, respectively. NE1 in the tryptophan ring of residue 63 and lying approximately perpendicular to the polar face of the NAG ring in bulgecin, makes a hydrogen bond with O15. Similar interactions are seen in the chito-oligosaccharide–RBTL complexes (Karlsen & Hough, 1995). O14 makes a hydrogen bond to water 150 (see Fig. 6), and another is found between O33 and water 243 which in turn is hydrogen bonded to OD2 of Asp103. Another water-mediated network of hydrogen bonds is seen between the sulfate group and the main-

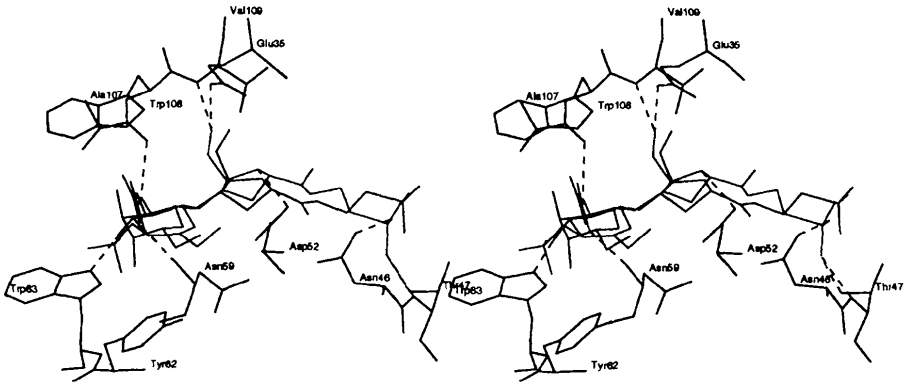

Fig. 5. A superimposition of the free (green) and the liganded form (red) of bulgecin in the active site of RBTL (blue).

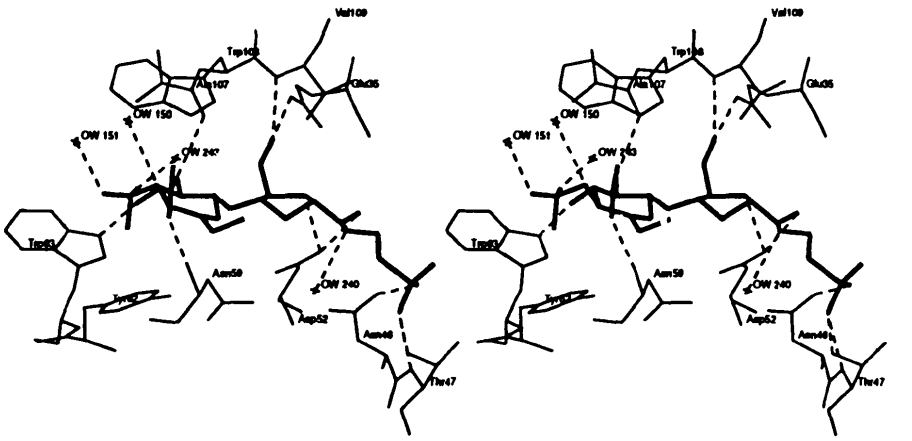

Fig. 6. Hydrogen-bonding interactions between RBTL and bulgecin. The lysozyme structure is shown with thin lines, bulgecin with thick lines and hydrogen bonds with broken lines. Water molecules are depicted with crosses.

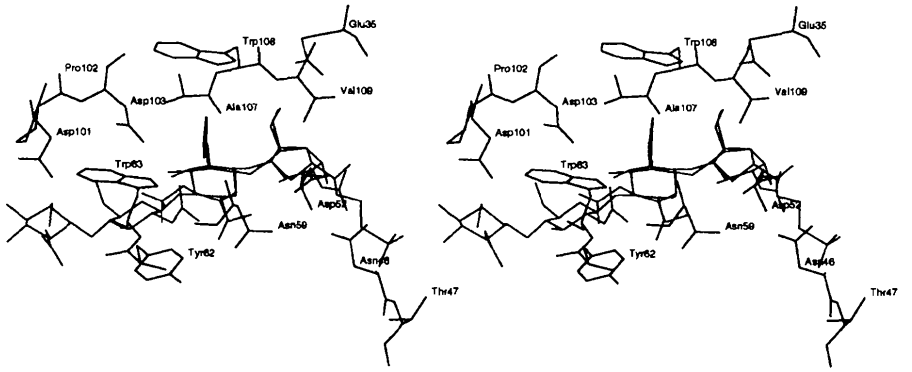

Fig. 7. A superimposition of the bound bulgecin molecule (green) and $(NAG)_4$ (red) in the active site of RBTL (blue).

chain CO groups of Val98 and Val104. Water 151 is hydrogen bonded to O34 and to water 153 which makes two further hydrogen bonds to the protein.

The proline ring of bulgecin binds in the same way to subsite *D* as the equivalent NAG unit in the RBTL–$(NAG)_4$ complex. In Fig. 7, a superimposition of the bulgecin and $(NAG)_4$ molecules in the active site, illustrates that the hydroxymethyl group of the proline ring in bulgecin occupies the same position as the hydroxymethyl group of the NAG ring. O22 in the C11 hydroxymethyl group of the proline ring makes two hydrogen-bonded interactions with the lysozyme; one to the main-chain NH of Val109 and the other to the OE2 atom of the catalytic residue Glu35. The same interactions, from the O6 atom in the C5 hydroxymethyl group, are found in the chito-oligosaccharide–RBTL complexes (Karlsen & Hough, 1995). N7 in the proline ring is hydrogen bonded to the ionized OD2 of Asp52. The equivalent interaction with an oligosaccharide substrate is believed to stabilize the positively charged carbonium ion in the transition state (Phillips, 1966; Blake *et al.*, 1967). A similar hydrogen bond between the endocyclic O5 of the NAG ring bound to site *D* in RBTL was found for the tri- and tetra-oligomers of chitin (Karlsen & Hough, 1995).

The taurine moiety, which is the most flexible part of the bound bulgecin molecule, is bound to the left side of the active-site cleft with the sulfonyl group making three hydrogen-bonded contacts to OG1 of Thr47, the NH group of Thr47 and ND2 of Asn46 (See Table 4). This locks the taurine 'tail' in position. The last hydrogen bond in the RBTL–bulgecin complex, is seen between N25 and water 240.

A simple extension of the bound tetra-NAG molecule in RBTL with two more NAG units also indicated a 'left-sided' binding mode (Banerjee, Holler, Hess & Rupley, 1975) to the lower part of the active-site cleft (Karlsen & Hough, 1995). Fig. 8 which illustrates the observed binding mode for bulgecin and the proposed binding mode for $(NAG)_6$, shows that both molecules interact with residues in the β-sheet region (residues 44, 46 and 47).

The proline ring of bulgecin is, as are the site *D* sugar units in the RBTL–saccharide complexes, not as close to the catalytic glutamic acid in the active site as is the distorted NAM moiety for MGM in HEWL (Strynadka & James, 1991). These results give support to conformational energy calculations on HEWL using the homopolymer $(NAG)_6$ (Pincus & Scheraga, 1979) and a copolymer of alternating NAG and NAM residues (Pincus & Scheraga, 1981), which suggest that the mode of binding of the saccharides to subsites *E* and *F* in the lower part of the active-site cleft in enzyme–substrate complexes depends on the conformation and binding mode of the sugar unit in subsite *D*. In the 'left-sided' binding mode which is most stable, the *D*-site saccharide, positioned close to the surface of the cleft and somewhat removed from the catalytic residues, has the normal unstrained chair conformation. The fifth and sixth residues bind to sites *E* and *F* making contacts with Arg45, Asn46 and Thr47. In the higher energy 'right-sided' mode the *D*-site saccharide is located more deeply in the cleft near to Glu35 and Asp52 and units *E* and *F* make contacts with residues Phe34 and Arg114. A third low-energy structure, with a 'right-sided' binding mode and a distorted ring in site *D*, is found to optimize the protein–sugar contacts in sites *E* and *F*.

From the observed position of the proline ring in bulgecin and from conformational energy calculations (Pincus & Scheraga, 1979, 1981), it seems reasonable to expect, as we indeed observe, a 'left-sided' binding mode in of the taurine moiety of bulgecin in the lower part of the cleft. However, since the taurine moiety of bulgecin has a completely different geometry and needs less space than two *N*-acetylglucosamine units, conclusions from these results must be exercised with caution.

3.5. *Changes in temperature factors for RBTL*

Average temperature factors for protein atoms in native RBTL and the RBTL–bulgecin complex are 26.3 and 27.2 Å^2, respectively, with corresponding values for the main-chain atoms 22.0 and 21.9 Å^2. These results imply that the lysozyme molecule does not become more ordered upon binding of the bulgecin molecule. A *B*-factor plot seen in Fig. 9, shows a comparison of mean backbone temperature factors along the polypeptide chain for native and liganded lysozyme. In common with the native structure, the areas that exhibit the

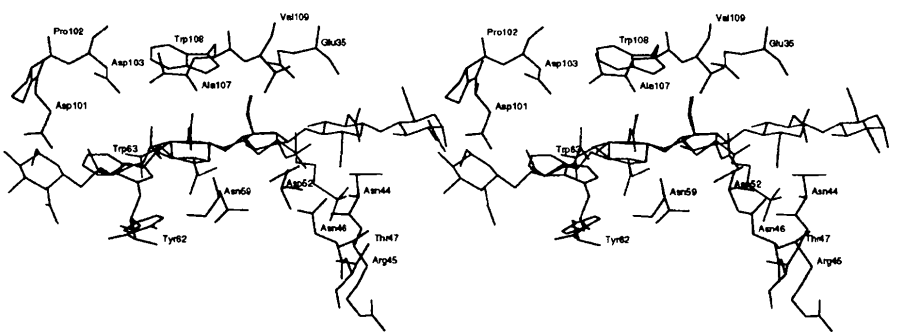

Fig. 8. A comparison of bulgecin (green) and $(NAG)_6$ (red) in the active site of RBTL. The mode of binding of the sugar rings in sites *E* and *F* was modelled from the crystallographically determined position of $(NAG)_4$ (Karlsen & Hough, 1995).

highest flexibility are found in the external loop regions from residues 45 to 50 which form a β-bend in the three-stranded β-sheet area, residues 60–73 in a long coiled loop and residues toward the C terminus.

The *B*-factor plot indicates that the mobility of the residue 45–50 loop is reduced on binding bulgecin. Asn46 and Thr47 in this loop are hydrogen bonded to the sulfonyl group of bulgecin. The residue 60–73 loop shows only a slight, possibly non-significant, reduction in mobility. In general, the rainbow trout lysozyme does not exhibit the same decrease in mobility in the active-site region upon binding of bulgecin as was seen in complexes RBTL–$(NAG)_4$ (Karlsen & Hough, 1995) and HEWL–MGM (Strynadka & James, 1991). One explanation for this may be that the oligosaccharides are more extensively bonded to the lysozymes by hydrogen-bonding and van der Waals interactions than is the bulgecin molecule.

3.6. *Conformational changes in RBTL*

The atomic coordinates of the native rainbow trout lysozyme were compared with those of the lysozyme molecule in complex with bulgecin. The r.m.s. deviations between the native and liganded structures for main-chain and all protein atoms are 0.12 and 0.40 Å, respectively, indicating only small conformational changes upon binding of the bulgecin molecule.

R.m.s. differences for backbone atoms of the native and bulgecin bound RBTL are seen in Fig. 10. The plot emphasizes that in addition to the C-terminal end which is quite flexible in both liganded and unliganded forms, there is one specific region, from residues 103 to 119, that exhibits the greatest conformational differences. Val109, in the middle of the 104–114 α-helix, is directly involved in the binding of bulgecin, which probably moves the α-helix closer to the bound inhibitor. The same region was also found to move significantly on formation of the RBTL–$(NAG)_4$ complex (Karlsen & Hough, 1995).

Smaller conformational changes in the complex between RBTL and bulgecin are seen in the short loops from residues 19 to 23, 45 to 50 and 69 to 73. The latter of these three regions (Thr69–Lys73) packs against the Asn59–Cys64 binding loop, but does not participate directly in interactions with the bulgecin molecule. In the residue 59–64 binding loop, both Asn59 and Trp63 are hydrogen bonded to bulgecin, but do not exhibit any significant shift in position. The second of the loops mentioned above (45–50), where Asn46 and Thr47 are involved in substrate binding, shifts in position as well as becoming more ordered. The 19–23 loop, which is not part of the active-site cleft but lies on the surface of the lysozyme molecule, presumably shows change in position due to high flexibility.

The present crystallographic results together with previously solved complexes of liganded forms of RBTL (Karlsen & Hough, 1995), correlate well with theoretical prediction which suggests that the two domains in lysozyme move as rigid bodies with a hinge motion which slightly opens and closes the active-site cleft to partially bury the substrate molecules (Brooks & Karplus, 1985; Gibrat & Gö, 1990). In general, positional changes around the active site of RBTL when complexed with bulgecin, seem to be less extensive than the shifts in atomic positions upon binding of the $(NAG)_4$ molecule.

4. Concluding remarks

From an analysis of the refined structure of the complex between RBTL and bulgecin, we can conclude

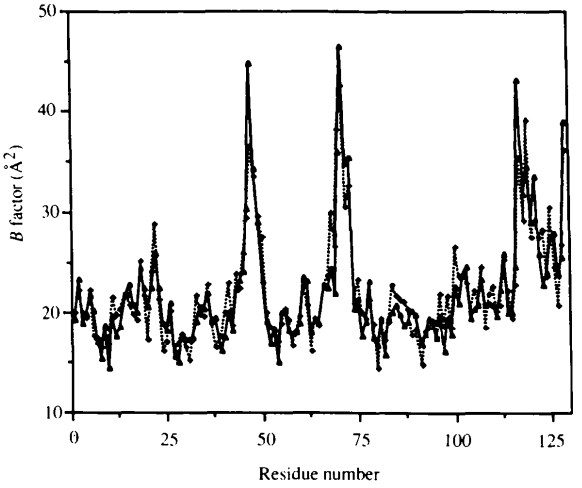

Fig. 9. Variation in isotropically temperature factors [B (Å^2)] averaged over main-chain atoms along the polypeptide chain for the native (unbroken lines) and bulgecin bound structures (broken lines) of RBTL.

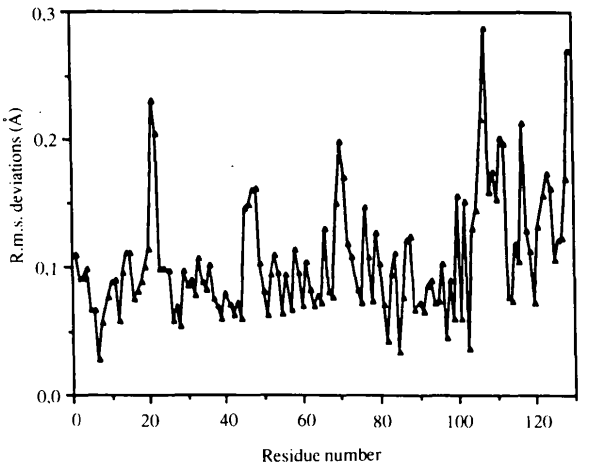

Fig. 10. R.m.s. differences along the main-chain atoms between the native and the bulgecin bound structure of RBTL.

that the bulgecin molecule in common with the chito-oligosaccharides in complex with RBTL (Karlsen & Hough, 1995) binds to the active-site cleft by an extensive network of hydrogen bonds. As in the SLT–bulgecin complex (Thunnissen *et al.*, 1994), the NAG ring of bulgecin is bound to subsite *C*, which is the most energetically preferred binding site and is important for substrate recognition and cleavage specificity of the glycosidic linkage (Imoto *et al.*, 1972). The proline ring of the bulgecin molecule is found in subsite *D* with the taurine moiety pointing toward the left side of the 'lower' part of the active-site cleft and making hydrogen-bonded interactions with Asn46 and Thr47 in the β-bend loop region. This result gives support to a 'left-sided' mode of binding of the substrate (Banerjee *et al.*, 1975), although one should be aware of that the structure of bulgecin is quite different from the natural cell wall substrate.

The proline-ring residue, buried into site *D* and hydrogen bonded to the catalytically active residues, Glu35 and Asp52, seems to have the 'normal' conformation. Since this ring is linked to the taurine moiety by a peptide bond and not a glycosidic linkage, bulgecin is not hydrolysed by lysozyme. It seems, therefore, reasonable to believe that, as for the soluble lytic transglycosylase from *E. coli* (Thunnissen *et al.*, 1994), bulgecin might be an inhibitor for rainbow trout lysozyme and probably other lysozymes. These results imply that bulgecin together with β-lactam antibiotics, causes bulge formation in bacteria by inhibiting the muramidases which are responsible for the partial degradation and reorganization of the cell walls glycan strands. The observation that bulgecin shows no antibacterial effect itself, suggests that the cell walls first have to be damaged by the β-lactam antibiotics which block the PBP's involved in cell wall synthesis, and, thus, rendering the polysaccharide chains more accessible to lysozyme.

Penicillin and other β-lactam antibiotics do not inhibit enzymes that act solely on the glycosidic bonds in the glycan strands (Waxman & Strominger, 1983). The crystal structures of RBTL and the soluble lytic transglycosylase from *E. coli* might, therefore, be used for the design of novel antibiotics which inhibit the murein hydrolases, but are distinct from the β-lactams.

This work is supported by the Norwegian Research Council (NFR), and we thank Takeda Industries Ltd, Japan, for providing us with the bulgecin compound and the atomic coordinates, and Dr Bjorn Grinde, National Institute of Public Health, Oslo, for the purified rainbow trout lysozyme.

References

Banerjee, S. K., Holler, E., Hess, G. P. & Rupley, J. A. (1975). *J. Biol. Chem.* **250**, 4355–4367.

Blake, C. C. F., Johnson, L. N., Mair, G. A., North, A. C. T., Phillips, D. C. & Sarma, V. R. (1967). *Proc. R. Soc. London Ser. B*, **167**, 378–388.

Brooks, B. & Karplus, M. (1985). *Proc. Natl Acad. Sci. USA*, **82**, 4995–4999.

Cheetham, J. C., Artymiuk, P. J. & Phillips, D. C. (1992). *J. Mol. Biol.* **224**, 613–628.

Collaborative Computational Project, Number 4 (1994). *Acta Cryst.* D**50**, 760–763.

Dautigny, A., Prager, E. M., Pham-Dinh, D., Jollés, J., Pakdel, F., Grinde, B. & Jollés, P. (1991). *J. Mol. Evol.* **32**, 187–198.

Gibrat, J.-F. & Gö, N. (1990). *Proteins Struct. Funct. Genet.* **8**, 258–279.

Grinde, B., Jollés, J. & Jollés, P. (1988). *Eur. J. Biochem.* **173**, 269–273.

Hendrickson, W. A. (1985). *Methods Enzymol.* **115**, 252–270.

Höltje, J.-V., Mirelman, D., Sharon, N. & Schwarz, U. (1975). *J. Bacteriol.* **124**, 1067–1076.

Höltje, J.-V. & Schwarz, U. (1985). *Molecular Cytology of Escherichia coli*, pp. 77–119. London: Academic Press.

Imada, A., Kintaka, K., Nakao, M. & Shinagawa, S. (1982). *J. Antibiot.* **35**, 1400–1403.

Imoto, T., Johnson, L. N., North, A. C. T., Phillips, D. C. & Rupley, J. A. (1972). *The Enzymes*, Vol. VII, pp. 665–868. New York: Academic Press.

Jeffrey, G. A. (1990). *Acta Cryst.* B**46**, 89–103.

Jollés, P. & Jollés, J. (1984). *J. Mol. Cell. Biochem.* **63**, 165–189.

Jones, T. A. (1985). *Methods Enzymol.* **115**, 157–170.

Kabsch, W. (1988). *J. Appl. Cryst.* **21**, 67–71.

Karlsen, S., Eliassen, B. E., Hansen, L. Kr., Larsen, R. L., Riise, B. W., Smalås, A. O., Hough, E. & Grinde, B. (1995). *Acta Cryst.* D**51**, 354–367.

Karlsen, S. & Hough, E. (1995). *Acta Cryst.* D**51**, 962–978.

Kraulis, P. J. (1991). *J. Appl. Cryst.* **21**, 946–950.

Laskowski, R. A., MacArthur, M. W., Moss, D. S. & Thornton, R. M. (1993). *J. Appl. Cryst.* **26**, 283–291.

Luzzati, P. V. (1952). *Acta Cryst.* **5**, 802–810.

Mo, F. & Jensen, L. H. (1978). *Acta Cryst.* B**34**, 1562–1569.

Nakao, M., Yukishige, K., Kondo, M. & Imada, A. (1986). *Antimicrob. Agents Chemother.* **30**, 414–417.

Pflugrath, J. W. (1989). *MADNES, Munich Area Detector NE System User's Guide*. Cold Spring Harbor Laboratory.

Phillips, D. C. (1966). *Sci. Am.* **215**, 78–90.

Pincus, M. R. & Scheraga, H. A. (1979). *Macromolecules*, **12**, 633–644.

Pincus, M. R. & Scheraga, H. A. (1981). *Biochemistry*, **20**, 3960–3965.

Rogers, H. J., Perkins, H. R. & Ward, J. B. (1980). *Microbial Cell Walls and Membranes*, pp. 190–214. London: Chapman and Hall.

Shinagawa, S., Kasahara, F., Wada, Y., Harada, S. & Asai, M. (1984). *Tetrahedron*, **40**, 3465–3470.

Shinagawa, S., Maki, M., Kintaka, K., Imada, A. & Asai, M. (1985). *J. Antibiot.* **38**, 17–23.

Spratt, B. G. (1975). *Proc. Natl Acad. Sci. USA*, **72**, 2999–3003.

Strynadka, N. C. J. & James, M. N. G. (1991). *J. Mol. Biol.* **220**, 401–424.

Templin, M. F., Edwards, D. H. & Höltje, J.-V. J. (1992). *Biol. Chem.* **267**, 20039–20043.

Thunnissen, A.-M. W. H., Dijkstra, A. J., Kalk, K. H., Rozeboom, H. J., Engel, H., Keck, W. & Dijkstra, B. W. (1994). *Nature (London)*, **367**, 750–753.

Waxman, D. J. & Strominger, J. L. (1983). *Ann. Rev. Biochem.* **52**, 825–869.